



Kinnunen-Grubb, M., Sapkota, R., Vignola, M., Nunes, I. M. and Nicolaisen, M. (2020) Breeding selection imposed a differential selective pressure on the wheat root-associated microbiome. *FEMS Microbiology Ecology*, 96(11), fiae196.  
(doi: [10.1093/femsec/fiae196](https://doi.org/10.1093/femsec/fiae196))

There may be differences between this version and the published version. You are advised to consult the publisher's version if you wish to cite from it.

<http://eprints.gla.ac.uk/230461/>

Deposited on 1 March 2021

Enlighten – Research publications by members of the University of Glasgow  
<http://eprints.gla.ac.uk>

1 **Breeding selection imposed a differential selective pressure on the**  
2 **wheat root-associated microbiome**

3

4 Marta Kinnunen-Grubb<sup>1\*\*</sup>, Rumakanta Sapkota<sup>2\*\*</sup>, Marta Vignola<sup>3</sup>, Inês Marques Nunes<sup>1</sup>, Mogens  
5 Nicolaisen<sup>4\*</sup>

6

7 <sup>1</sup> Novozymes A/S, Microbiomics and Microbe Discovery Denmark, Biologiens Vej 2, 2800 Kgs.  
8 Lyngby, Denmark

9 <sup>2</sup> Aarhus University, Department of Environmental Science, Frederiksborgvej 399, 4000 Roskilde,  
10 Denmark

11 <sup>3</sup> University of Glasgow, School of Engineering, 78 Oakfield Ave, Glasgow G12 8LS, United  
12 Kingdom

13 <sup>4</sup> Aarhus University, Department of Agroecology, Forsøgsvej 1, 4200 Slagelse, Denmark

14

15

16

17 \*Correspondence: mn@agro.au.dk

18 \*\*These authors contributed equally to this manuscript

19

## 20 **Abstract**

21 Plants-microbiome associations are the result of millions of years of co-evolution. Due to  
22 breeding-accelerated plant evolution in non-native and highly managed soil, plant-microbe links  
23 could have been lost. We hypothesized that post-domestication breeding of wheat changed the  
24 root-associated microbiome. To test this, we analyzed root-associated fungal and bacterial  
25 communities shortly after emergence of seedlings representing a transect of wheat evolution  
26 including modern wheat, landraces, and ancestors. Numbers of observed microbial taxa were  
27 highest in landraces bred in low-input agricultural systems, and lowest in ancestors that had  
28 evolved in native soils. The microbial communities of modern cultivars were different from those  
29 of landraces and ancestors. Old wheat accessions enriched *Acidobacteria* and *Actinobacteria*,  
30 while modern cultivars enriched OTUs from *Candidatus Saccharibacteria*, *Verrucomicrobia* and  
31 *Firmicutes*. The fungal pathogens *Fusarium*, *Neosascochyta* and *Microdochium* enriched in  
32 modern cultivars. Both bacterial and fungal communities followed a neutral assembly model when  
33 bulk soil was considered as the source community, but accessions of the ancient *Triticum*  
34 *turgidum* and *T. monococcum* created a more isolated environment in their roots. In conclusion,  
35 wheat root-associated microbiomes have dramatically changed through a transect of breeding  
36 history.

37 **Keywords:** Breeding, Microbiome, Root, Wheat, Bacteria, Fungi, Selective pressure.

## 39 **Background**

40 Plants are colonized by massive diversity of microorganisms and the rhizosphere is considered  
41 one of the most active microbiological environments on Earth (Berendsen *et al.*, 2012). These  
42 plant-microbiome associations are the result of millions of years of co-evolution (Baltrus, 2017),  
43 and it is well documented that host genotype has significant, albeit minor, effects on microbial  
44 community composition, both aboveground (Sapkota *et al.*, 2015) and belowground (Lundberg *et*  
45 *al.*, 2012, Peiffer *et al.*, 2013). Many plant-associated microorganisms are crucial for plant growth,  
46 nutrient acquisition, as well as protection against biotic and abiotic stresses (Finkel *et al.*, 2017).  
47 In contrast to natural evolution, domestication is a fast anthropological selection of crops, which,  
48 like natural selection, is based on genetic diversity and selection of desired traits. Modern  
49 breeding has further accelerated evolutionary processes with a focus on selection of fertilizer-  
50 responsive high-yielding and disease-resistant cultivars. In parallel, agriculture has undergone  
51 dramatic intensification during the last century with increasing agronomic management including  
52 higher levels of fertilizer and pesticide inputs. Considering breeding is a result of human-induced  
53 selection rather than natural evolution, our understanding of breeding-induced evolutionary

54 interactions between microbiota and plant traits is only emerging (Perez-Jaramillo *et al.*, 2018,  
55 Escudero-Martinez & Bulgarelli, 2019).

56 It is evident that modern wheat is a result of changes of the plant genome through hybridization  
57 events and modification of genes in the process of selection of desirable plant traits. Such  
58 selection pressure for high yield in combination with high-input agriculture and neglect of root  
59 processes and performance, may inadvertently have led to depletion of members of the root  
60 microbiota that were important for nutrient acquisition and pathogen control in natural low-input  
61 conditions (Perez-Jaramillo *et al.*, 2016, Kavamura *et al.*, 2020, Tkacz *et al.*, 2020). In common  
62 sunflower (*Helianthus annuus*) domestication affected fungal communities, but not bacterial  
63 communities, and modern sunflower varieties had a lower relative abundance of putative fungal  
64 pathogens (Leff *et al.*, 2017). Similarly, bacterial isolates from sugar beet roots (*Beta vulgaris* ssp.  
65 *vulgaris*) were more active against phytopathogens, compared to isolates from the wild ancestor  
66 (*B. vulgaris* ssp. *maritima*), whereas isolates from wild beet showed higher ability to cope with  
67 abiotic stresses (Zachow *et al.*, 2014). The rhizomicrobiome of wild rice was less sensitive to  
68 introduction of a fungal pathogen and an introduced pathogen had lower abundance in wild rice  
69 (Shi *et al.*, 2018). In barley, a small but significant effect of domestication was manifested mainly  
70 on the abundance of several OTUs from various taxa, rather than on single OTUs (Bulgarelli *et*  
71 *al.*, 2015). In contrast, domestication effects were abundant in foxtail millet (*Setaria italica*) and its  
72 wild ancestor (*S. viridis*), including effects on Betaproteobacteria and Firmicutes, which were  
73 enriched in *S. italica* (Chaluvadi & Bennetzen, 2018). In wild and domesticated *Phaseolus*  
74 *vulgaris*, a gradual decrease in relative abundance of members of Bacteroidetes, and an increase  
75 of members of Actinobacteria and Proteobacteria was observed from wild to modern accessions  
76 (Perez-Jaramillo *et al.*, 2017). The evolutionary history of Poaceae (maize, sorghum, wheat and  
77 teosinte) was shaping bacterial communities, and increases in phylogenetic distance were  
78 reflected in increasing differences between microbial communities (Bouffaud *et al.*, 2014).

79 Modern wheat cultivars are the product of at least 10,000 years of human selection. Modern bread  
80 wheat (*Triticum aestivum* L.) has an allo-hexaploid genome consisting of three subgenomes  
81 (AABBDD) resulting from hybridization events between *T. urartu* (AA genome) and a close relative  
82 to *Aegilops speltoides* (BB genome), and a later hybridization with the wild diploid *A. tauschii* (DD  
83 genome) (Pont *et al.*, 2019). *T. turgidum* ssp. *dicoccoides* and *T. turgidum* ssp. *dicoccum* are allo-  
84 tetraploid emmer wheat varieties (BBAA genomes) that are suggested as direct progenitors of  
85 modern wheat (Avni *et al.*, 2017). Domesticated emmer, *T. turgidum* ssp. *dicoccum*, was first  
86 cultivated in the fertile crescent around 10,000 BCE. Einkorn, *T. monococcum* ssp. *monococcum*  
87 and *T. monococcum* ssp. *aegilopoides* are diploid species with AA genomes, also cultivated in

88 the fertile crescent (Abbasov *et al.*, 2018). Spelt wheat (*T. triticum* ssp. *spelta*) represents a  
89 hexaploid (AABBDD) type of hulled wheat, characterized by adaptation to a wide range of  
90 environments (Dinu *et al.*, 2018). Several wheat traits have changed dramatically during  
91 domestication such as root architecture and exudation of primary and secondary metabolites  
92 (Beleggia *et al.*, 2016, Rascio *et al.*, 2016, Iannucci *et al.*, 2017). This may have had profound  
93 effects on root and rhizosphere microbial communities, as demonstrated in a study of plant  
94 growth-promoting bacteria associated with roots of ancient and modern wheat (Valente *et al.*,  
95 2020). It has further been shown that modern wheat types are less dependent on arbuscular  
96 mycorrhizae than older types and that old accessions benefit more from mycorrhizal symbiosis  
97 (Kapulnik, 1991). It was suggested that this could be caused by the highly fertile conditions of soil  
98 during breeding and cultivation of modern cultivars (Hetrick *et al.*, 1993).

99 Understanding assembly processes of root-associated microbial communities, and their diversity  
100 and ecology may enhance future breeding programs. Here, we hypothesized that the  
101 modifications of the wheat genome occurring through 10,000 years of diversification resulted in a  
102 cognate selective pressure on the root-associated microbiota. To test our hypothesis, we selected  
103 three distinct genetic groups of Triticum depicting two major events in wheat evolutionary history.  
104 The genetically oldest group that we chose was Triticum accessions of *T. monococcum* (AA  
105 genome; *Tm*) and *T. turgidum* (BBAA genome; *Tt*). To represent the wheat *T. aestivum* (genome  
106 BBAADD), we included landraces grown before the 1940s and one accession of *T. triticum* ssp.  
107 *spelta*. Four commercial cultivars currently grown in Denmark were used as representing modern  
108 wheat. We grew those accessions under field conditions in agricultural soil and compared root  
109 fungal and bacterial communities in field plots at three time points shortly after emergence of the  
110 seedlings in the autumn. To examine the importance of deterministic versus stochastic processes  
111 in the assembly of root-associated microbial communities, we employed a neutral community  
112 assembly model (Sloan *et al.*, 2006).

113

## 114 **Methods**

### 115 **Soil and plant sampling**

116 Accessions of old wheat lines were provided by NordGen, Alnarp, Sweden  
117 (<https://www.nordgen.org/en/>). The untreated seeds of 5 accessions of wheat ancestors (*T.*  
118 *turgidum* ssp. *dicoccum* (*Tt*), *T. monococcum* ssp. *monococcum* (*Tm*) and *T. monococcum* ssp.  
119 *aegilopoides* (*Tm*)), 5 accessions of landraces (*T. aestivum* ssp. *aestivum*), one accession of *T.*  
120 *aestivum* ssp. *spelta* (*Tas*) and 4 modern wheat cultivars (*T. aestivum* ssp. *aestivum*) were sown  
121 on a sandy clay loam soil in the autumn 2017 in 50 cm rows at Aarhus University, Flakkebjerg,

122 Denmark (55.322631°N, 11.394336°E) (Table 1). No fungicide treatments were applied. For data  
123 analysis, all accessions were categorized as modern cultivars, landraces, *Tas* or wheat ancestors,  
124 *Tt* and *Tm* (Table 1).

125 For each cultivar, root samples including tightly attached soil, were collected destructively in  
126 quadruplicates at roughly BBCH10 (emergence of first leaf), BBCH12 (first leaf fully unfolded) and  
127 BBCH21 (first side shoot visible) (Lancashire *et al.*, 1991) during the autumn 2017 starting from  
128 October 31 (Table S1). Each root sample was a composite of four plants, which were randomly  
129 uprooted and carefully separated from loosely attached soil.

130 Bulk soil samples were collected from the plough layer (0-20 cm) in between crop rows at each  
131 sampling point. In each sampling line (space between two crop rows) 10 soil sub-samples were  
132 collected, thoroughly mixed and from those, two replicate composite bulk soil samples were  
133 collected (n=10). All samples were frozen at -80°C until further processing for DNA extraction.

134

#### 135 **Sample homogenization and DNA extraction**

136 Soil and root samples were freeze-dried for 48h at -111°C and 0.0026 Pa using a CoolSafe  
137 CS110-4 Pro freeze dryer (LaboGene, Denmark) and finely crushed using zirconium oxide  
138 grinding balls (10mm) and a Fast & Fluid Management shaker-SK350 (Fast & Fluid, Sassenheim  
139 Netherlands). DNA was extracted from homogenized soil and root samples using the  
140 NucleoSpin® DNA 96 Soil Kit (Macherey-Nagel GmbH & Co KG, Düren, Germany) adapted to a  
141 Biomek® FCP Laboratory Automation Workstation (Beckman Coulter™, CA, USA). Four negative  
142 controls (500µL of PCR graded water) were included per extraction plate and used for amplicon  
143 library preparation together with the samples. Concentration of extracted DNA was measured  
144 using a Qubit 3.0 fluorometer (Thermo Fisher Scientific, MA, USA) with a Qubit dsDNA HS Assay  
145 Kit (range 0.2-100ng; Invitrogen, Life Technologies). DNA was then stored at -20°C.

146

#### 147 **Amplicon library preparation and sequencing**

148 Extracted DNA was used to produce bacterial and fungal amplicon libraries (Table S2). The fungal  
149 ITS2 region was amplified using fITS7 and ITS4 primers (Ihrmark *et al.*, 2012) and the bacterial  
150 16S rRNA V3-V4 region was targeted using primers S-DBact-0341-b-S-17/S-D-Bact-0785-a-A-  
151 21 (Klindworth *et al.*, 2013). PCR was performed in a reaction mixture of 25 µl consisting of 1 ×  
152 PCR reaction buffer, 1.5 mM MgCl<sub>2</sub>, 0.2 mM dNTPs, 1 µM of each primer, 1 U of GoTaq Flexi  
153 polymerase (Promega Corporation, Madison, USA) and 1µl of DNA template. PCR was  
154 conducted in a GeneAmp PCR System 9700 thermal cycler (Thermo Fisher Scientific, MA, USA)  
155 using 94 °C for 5 min, followed by 25 cycles at 94 °C for 30 s, 55 °C for 30 s, 72 °C for 1 min, and

156 a final elongation step at 72 °C for 10 min. For fungal amplicon library preparation, an annealing  
157 temperature of 57 °C was used as recommended (Ihrmark *et al.*, 2012). For dual indexing, primers  
158 including indexing tags were used in a PCR for 10 cycles, with the thermal cycler program as  
159 described above. In addition to dual indexing, internal barcodes of varying length were added to  
160 the forward primer for combining samples within each index combination as described earlier (Wu  
161 *et al.*, 2015, Siddique & Unterseher, 2016). After PCR, amplicon size was confirmed by  
162 visualization in a 1.5% agarose gel using SYBR staining, PCR products were pooled, precipitated  
163 and re-eluted as described earlier (Sapkota & Nicolaisen, 2018). In order to remove primers and  
164 shorter reads, the pooled DNA was separated on a 1.5 % agarose gel and amplicons of the  
165 expected size (300–450 bp) were extracted using a QIAquick Gel Extraction Kit (Qiagen,  
166 Copenhagen, Denmark). The DNA concentration of the amplicon library was evaluated using a  
167 Qubit® Fluorometer (Thermo Fisher Scientific). Amplicon libraries were shipped to Eurofins MWG  
168 (Ebersberg, Germany) for sequencing on an Illumina MiSeq platform using a dual indexing  
169 strategy.

170

### 171 **Amplicon sequencing data analysis**

172 Quality processing and bioinformatics of the reads obtained from Illumina MiSeq were analysed  
173 as described earlier (Kudjordjie *et al.*, 2019). Briefly, paired end reads were filtered with Phred  
174 quality scores > 30 and merged with an overlapping minimum read length of 30 base pairs using  
175 VSEARCH v. 2.6 (Rognes *et al.*, 2016). Forward and reverse primers, as well as internal barcodes  
176 were trimmed and reads with less than 200 base pairs were excluded. Before clustering at 97%  
177 similarity, all reads were dereplicated and screened using VSEARCH. Taxonomy assignments  
178 for the clustered operational taxonomic units (OTUs) was done using SILVA v. 132 for bacteria  
179 and UNITE v. 8.0 for fungi in QIIME v 1.9, using assign\_taxonomy.py (Caporaso *et al.*, 2010,  
180 Quast *et al.*, 2013). OTUs unassigned at kingdom level or assigned as chloroplast or  
181 mitochondrial sequences were removed from the datasets. Furthermore, samples with less than  
182 2,000 reads were excluded from downstream analysis.

183 Bacterial and fungal annotation tables were analyzed in R v.3.5.2 (R Core Team, 2017), using  
184 the RStudio development environment (RStudio Team) and making use of the 'phyloseq' package  
185 (McMurdie & Holmes, 2013). The OTU tables were transformed, by either rarefaction or relative  
186 abundance, before executing diversity-based calculations. Alpha diversity was estimated using  
187 observed OTU richness and Shannon diversity measures, using the mean value from rarified  
188 OTU tables generated 100 times at a sampling depth of 3,000 reads per sample. Significant  
189 differences between diversity indices were determined using the Kruskal-Wallis rank sum test.

190 Bray-Curtis distance matrices were used for beta diversity analysis at OTU level using unrarefied  
191 data (all included samples with > 2,000 reads per sample) and transformed to relative abundance.  
192 Variance partitioning and significance for experimental factors were detected by PERMANOVA  
193 (R package: 'vegan'). Dissimilarity between samples (based on Bray-Curtis distances) was  
194 visualized using NMDS plots.

195

### 196 **Community assembly model**

197 To study the importance of selection versus neutral processes in community assembly, a modified  
198 version (Morris *et al.*, 2013) of the model described earlier (Sloan *et al.*, 2006) was applied. This  
199 neutral community assembly model (NCM) predicts the frequencies with which taxa should occur  
200 in target communities based on their abundance in the source community (also referred to as  
201 metacommunity). In short, the model predicts that abundant taxa in the source community will be  
202 observed more frequently in the target communities due to increased immigration opportunities,  
203 while rare taxa will more likely be lost in the target community due to ecological drift. The OTU  
204 table was transformed by rarefaction to 2000 reads per sample and normalization into relative  
205 abundances, before the analysis. The model fit is determined by the coupled parameter  $N_i * m$ ;  
206 where  $N_i$  is the size of the community (the number of reads in the samples was considered as an  
207 estimation of the community size);  $m$  is the migration rate. The migration rate is the estimated  
208 probability that the random loss of an individual in the local community will be replaced by  
209 immigration from the source community. The fitting of the model parameters was performed in R  
210 where binomial proportion 95% confidence intervals (based on the Wilson method) around the  
211 model predictions were calculated using the 'HMisc' package (Harrell, 2016). In this study, root  
212 samples were considered as local communities, while the composition of the source community  
213 was inferred by averaging the composition of the bulk soil samples. Among the local communities,  
214 two separate groups were identified: roots communities associated with the modern opposed to  
215 old cultivars; these two analyses were performed for the fungal and bacterial communities  
216 separately. OTUs falling between the 95% confidence interval were considered to be present as  
217 a result of neutral dynamics of birth, death and immigration from the source (bulk soil); OTUs  
218 falling outside the confidence interval (and with the ratio between observed frequency and  
219 predicted frequency greater than 1.5 or lower than 0.5) were found with frequencies  
220 disproportionally higher or lower than predicted by the model based on their abundances in the  
221 soil and therefore considered to be present in the communities as a result of deterministic factors.  
222 Pearson Correlation between the frequency of the sequence variants estimated by the model and  
223 that of observed was used to determine the statistical significance of model fit. The analysis was

224 performed considering only OTUs shared by the bulk soil community (source) and the root  
225 community (target). In this case, all sequence variants that were detected in the root, but not in  
226 the bulk soil, and vice versa were excluded, as it is routinely done (Morris *et al.*, 2013, Kinnunen  
227 *et al.*, 2017, Vignola *et al.*, 2018). The number of OTUs shared between target and source  
228 communities and employed in the model are shown in Table 3.

229

## 230 **Results**

### 231 **Amplicon sequencing quality**

232 Sequencing of the bacterial 16S rRNA amplicon library resulted in 8,806 OTUs in 210 samples  
233 (excluding controls). Number of reads per sample ranged between 0 and ~80,000 (Figure S1).  
234 Samples with less than 2,000 reads were removed from downstream analysis (n=16).  
235 Furthermore, 504 OTUs unclassified at kingdom level and 29 sequences classified as chloroplast  
236 at family level were removed from the dataset. After clustering, the length of representative  
237 sequences of 16S V3-V4 region was  $417 \pm 10$  bp (mean  $\pm$  sd). Therefore, 11 OTUs with  
238 sequences shorter than 390 bp were eliminated from the dataset (Figure S1). Sequencing of the  
239 fungal ITS amplicon library resulted in 561 OTUs in 210 samples (excluding controls). Number of  
240 reads per samples ranged between 0 and ~150,000 (Figure S1). Samples with less than 2,000  
241 reads were removed from the downstream analysis (n=10). Furthermore, 170 sequences not  
242 classified at kingdom level were removed from the analysis. Fourteen sequences smaller than  
243 135 bp were removed from the dataset (Figure S1).

244 Rarefaction curves indicated that the number of reads sampled the variation in fungal  
245 communities whereas bacterial variation was not covered completely in our sampling strategy  
246 (Figure S2).

247

### 248 **Community alpha diversity**

249 As expected, bulk soil alpha diversity was always higher than the alpha diversity of the root  
250 samples (Figure 1). Alpha diversity in roots increased from BBCH10 to BBCH21. Differences in  
251 alpha diversity among genetic groups, measured as observed species richness and Shannon  
252 diversity indices, were most pronounced at BBCH 10, whereas the alpha diversity approached  
253 similar levels at BBCH21. For both bacteria and fungi, Landraces + *Tas* had the highest alpha  
254 diversity of all accessions. *Tt* generally had the lowest alpha diversity, most clearly observed in  
255 the bacterial dataset.

256

### 257 **Microbial communities separate according to wheat evolution**

258 Comparative analysis of modern cultivars, Landraces + *Tas*, and ancient accessions (*Tm* and *Tt*)  
259 separated the groups in NMDS plots, but differently at the three growth stages. This indicates a  
260 significant effect of wheat genotypes and BBCH on the microbial community composition  
261 ( $p=0.001$  for each BBCH) (Figure 2, Figure S3). We observed clear separation of bulk soil  
262 microbial communities from the root communities of all wheat accessions, the latter being more  
263 dynamic over time. Although the root bacterial and fungal community composition shifted between  
264 growth stages, the separation of modern cultivars from Landraces + *Tas* and *Tt* and *Tm* was  
265 remarkable (Figure 2 and Table 2). We observed noticeable differences between the wheat  
266 genetic groups. Landraces + *Tas* clearly clustered at all growth stages while the microbial  
267 community composition of the roots of *Tt* became more similar over time and approached the  
268 other genetic groups, except the modern cultivars, indicating a stronger succession of microbial  
269 communities in the *Tt* roots than in the roots of *T. aestivum*.

270 Comparing the dynamics of bacterial and fungal communities, we observed a stronger selection  
271 on bacterial communities compared to fungal communities at the first growth stage (based on  
272 stronger clustering of samples). However, over time, selection in fungal communities increased.  
273 Fungal community composition in roots of ancient accessions was distinct from modern cultivars,  
274 and bacterial communities of modern cultivars were even more clearly separated from the  
275 landrace/ancient lines. Furthermore, overall fungal community composition in roots was similar to  
276 the bulk soil community composition, whereas the bacterial community composition in bulk soil  
277 clearly separated from root communities. PERMANOVA tests confirmed that both fungal and  
278 bacterial communities in soil and roots were significantly different in the total dataset ( $p<0.001$ ),  
279 confirming our observations of the NMDS plots (Table 2). When root associated microbial data  
280 was split according to growth stage, the different wheat groups had significantly different  
281 communities ( $p<0.001$ ; fungi at BBCH21,  $p<0.01$ ). However, the wheat genetic groups explained  
282 a higher proportion of the variation in bacterial communities.

283

#### 284 **Taxa significantly enriched in the roots of old and modern wheat lines**

285 For this analysis, we grouped the wheat lines into old (*Tm*, *Tt*, landraces and *Tas*) and modern  
286 lines (KWS Desanto, Substance, Sherif and Torp). We observed differences in taxa enriched in  
287 the roots of old and modern communities (Figure 3, Figure S4-S6). The most remarkable  
288 differences in bacterial enrichment could be accounted to OTUs belonging to *Acidobacteria* and  
289 *Actinobacteria* primarily in old cultivars at BBCH21, while modern cultivars enriched OTUs from  
290 *Saccharibacteria*, *Verrucomicrobia* and *Firmicutes* (Figure 3a). Furthermore, modern cultivars  
291 had higher numbers of enriched OTUs of *Bacteroidetes* at BBCH10, but this effect was absent at

292 BBCH21. We also observed phylum level differences of fungal taxa enriched in the roots (Figure  
293 3b). Taxa belonging to *Ascomycota* and *Basidiomycota* were enriched in both old and modern  
294 cultivars, but the number of enriched *Basidiomycota* was much higher in the old wheat lines.  
295 Although at a low number (and abundance), *Mortierellomycota*, *Olpidiomycota* and  
296 *Chytridiomycota* taxa were solely enriched in the roots of old cultivars. At OTU level, we observed  
297 a stronger enrichment of bacterial families in the modern cultivars compared to ancient lines  
298 (Figure S5a). Interestingly, similar patterns were not observed for the fungal communities (Figure  
299 S5b). Modern wheat cultivars strongly enriched for OTUs belonging to *Rhizobiaceae*,  
300 *Flavobacteriaceae* and *Pedobacter*. The most significantly enriched family in the communities of  
301 the old lines was *Sphingomonadaceae* (Figure S6a). *Microdochium*, *Neosascochyta*,  
302 *Sporobolomyces* and *Fusarium* were enriched in modern cultivars whereas basidiomyceteous  
303 yeasts such as *Filobasidium*, *Holtermanniella* and *Psathyrella*, and the ascomycete *Aureobasidium*  
304 were enriched in the old lines (Figure S6b). Surprisingly, we observed that genera within  
305 *Basidiomycota* were more frequently enriched (and with higher significance) in old lines, while  
306 *Ascomycota* dominated in the modern cultivars.

307

### 308 **What drives the community assembly in the roots of wheat?**

309 Bacterial communities from both modern and old wheat accessions showed very strong  
310 correlation with the neutral model (NCM) (Sloan *et al.*, 2006) when the bulk soil community was  
311 considered as the source (Figure 4). The model explained 75% and 78% (Pearson correlation) of  
312 the observed variation in the frequencies of OTUs present in the local bacterial communities  
313 associated with modern and old lines, respectively (Table 3). Fungal communities also correlated  
314 strongly with the model: a Pearson correlation value of 0.86 was observed for the modern  
315 community and 0.87 for the ancient community (Table 3). The immigration rates for the bacterial  
316 and fungal communities were estimated from the model (Ntm value used to fit the model with the  
317 observations divided by 2000 reads): 7.8% and 7.6% of the deaths happening in bacterial  
318 communities from modern and old accessions were replaced by OTUs from the source. Lower  
319 values were observed for the fungal communities: 3.0% and 4.8% for the modern and old  
320 community, respectively. Among the old cultivars, we distinguished two further subsets: *T.*  
321 *aestivum* landraces including *Tas*, and *T. monococcum* and *T. turgidum* lines. The migration rates  
322 for these two subsets of bacterial communities were 9.1% and 6.1%, respectively. Results  
323 suggest that among old accessions, *Tm* and *Tt* lines created a more isolated environment where  
324 fewer deaths happening within the local community were replaced by immigrants from the source  
325 community, compared to the environment created by the *T.aestivum* landraces.

326

## 327 **Discussion**

328 The goal of this study was to identify potential evolutionary ‘post-domestication breeding-effects’  
329 in wheat by comparing root microbial communities in three distinct genetic groups of *Triticum*  
330 depicting major events in the evolutionary history of wheat: modern cultivars, landraces and  
331 ancestors of wheat. Breeding for higher yields in high-input agriculture may inadvertently have  
332 led to depletion of beneficial microbial taxa associated with plant roots. For example, it was found  
333 that ancient wheat varieties were more capable of interacting with beneficial plant growth-  
334 promoting rhizobacteria (Valente *et al.*, 2020). Generally, the magnitude of genotype effects on  
335 microbial communities is significant but small (Peiffer *et al.*, 2013, Sapkota *et al.*, 2015, Wagner  
336 *et al.*, 2016). While a number of studies have investigated genotype effects in modern crop plants,  
337 fewer studies have specifically investigated long-term evolutionary effects by comparing modern  
338 crops and ancestors of those crops (Zachow *et al.*, 2014, Bulgarelli *et al.*, 2015, Leff *et al.*, 2017,  
339 Chaluvadi & Bennetzen, 2018, Brisson *et al.*, 2019). In the present study, we demonstrated effects  
340 of long-term breeding processes on root-associated microbial diversity, and we demonstrated that  
341 bacterial and fungal communities differed in a transect of evolution between the different groups  
342 of wheat: modern cultivars, landraces (including *T. triticum* ssp. *spelta*) and wheat ancestors (*T.*  
343 *turgidum* ssp. *dicoccum*, *T. monococcum* ssp. *monococcum* and *T. monococcum* ssp.  
344 *aegilopoides*). We were able to identify enriched bacterial and fungal taxa in old and modern  
345 wheat accessions, and we demonstrated that modern cultivars followed a neutral community  
346 assembly model to a higher degree than old lines, suggesting that the old lines posed a stronger  
347 selection on microbial community assembly.

348 Bacterial and fungal alpha diversity in bulk soil was higher than in root-associated communities,  
349 as has also been observed in numerous other studies, e.g. (Berendsen *et al.*, 2012). Both  
350 bacterial and fungal alpha diversity in root samples were generally lowest at BBCH10 and then  
351 dramatically increased and approached similar diversity levels at BBCH21. Similarly, rapid  
352 colonization of rice roots was demonstrated even after a few days following transplantation of  
353 seedlings to soil, and succession of communities that stabilized after 2 weeks of plant growth  
354 (Edwards *et al.*, 2015). Overall, our results show that there is a rapid initial microbial colonization  
355 phase from bulk soil to the root, and we speculate that this period is of high importance in shaping  
356 community structures in plant roots, also at the later stages of growth.

357 Bacterial colonization of roots of modern cultivars occurred faster than in wheat ancestors (*Tm*  
358 and *Tt*), indicating that wheat ancestors subject stronger selection on bacteria at the initial growth  
359 stages. On the other hand, the lowest diversity of fungal communities was observed in modern

360 cultivars at BBCH10. We speculate that one reason for this difference between bacterial and  
361 fungal communities could be that focus in plant breeding has been on fungal pathogens and that  
362 the plant immune system has been tuned to prevent fungal invasion. Thus, modern cultivars may  
363 be more selective towards fungi from the earliest stages of root development, inhibiting rapid  
364 stochastic colonization. The highest diversities of both bacteria and fungi were observed in the  
365 wheat landraces, as was also observed in other studies (Germida, 2001, Szoboszlay *et al.*, 2015).  
366 Landraces have been adjusted to agricultural settings during selection, whereas wheat ancestors  
367 *Tm* and *Tt* have been harvested from native soil and are thus not adjusted to the microbial  
368 communities found in modern agricultural soil. At the same time, landraces were bred in low-input  
369 soil in opposite to modern cultivars that have been bred in high-input soil, promoting lower  
370 dependency on microbial interactions in the root.

371 Both fungal and bacterial communities differentiated according to bulk soil and wheat type  
372 (modern, landrace + *Tas* or ancient (*Tm* and *Tt*)) in NMDS plots. Bulk soil communities separated  
373 from root communities over time, with the most remarkable separation observed at BBCH21. We  
374 observed a stronger selection of bacterial and fungal communities at the later growth stages  
375 based on the more distinct clustering of samples at BBCH21. Landraces and ancient lines of  
376 wheat clustered more distinctly at later stages, which could indicate a stronger selection during  
377 the colonization of ancient lines, as was also observed in a recent study (Hassani *et al.*, 2020).  
378 This study suggested stochastic processes are of higher importance in modern wheat lines  
379 compared to ancient lines and that domestication could have entailed less selective constraints  
380 on plant traits that contribute to microbial assembly. Bacterial communities clustered more  
381 distinctively at BBCH10 and BBCH12 compared to fungal communities suggesting a stronger  
382 selection of bacteria at the initial stages of colonization. Fungal and bacterial communities in the  
383 ancient wheat accessions clearly separated from modern cultivars already at BBCH10, showing  
384 that effects of breeding are manifested already at the initial growth stages of the wheat seedlings.  
385 Also of notice, both bacterial and fungal communities in modern cultivars separated from the  
386 communities in ancient and landrace accessions.

387 Several bacterial and fungal taxa were enriched in old or modern accessions. We noted that more  
388 members of *Acidobacteria* and *Actinobacteria* were enriched in the old accessions, while more  
389 OTUs from *Candidatus Saccharibacteria*, *Verrucomicrobia* and *Firmicutes* were enriched in the  
390 modern cultivars. Interestingly, most of these OTUs were predominantly enriched in BBCH21.  
391 *Acidobacteria*, *Verrucobacteria* and *Actinobacteria* are typically found in high abundance in the  
392 soil and rhizosphere, and plant roots selectively enrich for certain groups of *Acidobacteria* and  
393 *Verrucobacteria* (Nunes da Rocha *et al.*, 2013). *Actinobacteria* and *Firmicutes* are associated with

394 soil suppressiveness (Mendes *et al.*, 2011) and may thus be recruited as antagonists against soil-  
395 borne pathogens. At a lower taxonomic level, *Rhizobiaceae*, *Flavobacteriaceae* and *Pedobacter*  
396 were all enriched in modern cultivars. Interestingly, these taxa have all been suggested to have  
397 plant beneficial properties and to be enriched in the roots or rhizosphere of cereals (Yin *et al.*,  
398 2013, Poole *et al.*, 2018, Carrion *et al.*, 2019). Further corroborating this, a comparative study of  
399 microbiomes of cultivated sugar beet and its wild ancestor *Beta vulgaris* ssp. *maritima* found that  
400 a higher proportion of isolates that were active against phytopathogens in domesticated sugar  
401 beet (Zachow *et al.*, 2014). Likewise, higher amounts of *Flavobacteriaceae* in the roots and  
402 rhizosphere of a modern barley cultivar compared to the ancestor *Hordeum vulgare* ssp.  
403 *spontaneum* were found (Bulgarelli *et al.*, 2015). We observed enrichment of several known  
404 fungal wheat pathogens such as *Fusarium*, *Neosascochyta* and *Microdochium* in the modern  
405 cultivars. *Fusarium* was also enriched in roots of modern cultivars of sunflower compared to non-  
406 domesticated sunflower (Leff *et al.*, 2017). Whether enrichment of certain putative fungal  
407 pathogens in modern cultivars represents a general trend is unknown, but it is tempting to  
408 speculate that domesticated wheat may have lost the ability to prevent certain soil-borne  
409 pathogens, as those pathogens are not important in modern agricultural systems including  
410 efficient crop rotations.

411 Both bacterial and fungal communities of the roots of wheat fitted the neutral community assembly  
412 model very well suggesting that stochastic factors of birth, death and immigration from the bulk  
413 soil are largely driving the composition of both bacterial and fungal communities associated with  
414 wheat roots. The migration rates for landraces + *Tas* were higher compared to the ancient lines  
415 *Tm* and *Tt* (9.1% vs. 6.1%). This suggests that *Tm* and *Tt* lines created a more isolated  
416 environment from the soil compared to the environment created by landraces. Rossmann *et al.*  
417 (2020) observed stronger interactions in landraces with their soil microbiomes compared to  
418 modern wheat. Hassani *et al.* (2020) found a higher stochasticity in the assembly of microbial  
419 communities in modern wheat compared to the two ancestors *T. boeoticum* and *T. urartu*. With a  
420 lower immigration rate, we also expected lower alpha diversity, and indeed, we observed that *Tm*  
421 and *Tt* had the lowest alpha diversity. The high diversity of the soil was lost in the local root  
422 communities and the more the local communities were isolated (low immigration rates) the less  
423 diversity we observed (Rosindell *et al.*, 2011).

424 The results of our study suggest that changes have occurred during the process of breeding in  
425 the ability of wheat to assemble fungal and bacterial root communities. Whether these changes  
426 are a result of the selection for certain wheat traits under high nutrient availability remains an open  
427 question. It also remains to be elucidated whether such selection has led to changes in the ability

428 of wheat to cope with environmental stresses, to take up nutrients from the soil more efficiently  
429 and to avoid pathogens in the root more effectively. However, indications of less dependency in  
430 modern wheat on microbial interactions have emerged. Similarly, wheat dependence of  
431 mycorrhizal interactions was higher in landraces compared to ancestors and modern lines, and  
432 responsiveness to mycorrhizal colonization was lower in modern cultivars (Schmidt *et al.*, 2016).  
433 In conclusion, we have demonstrated remarkable effects of human-induced evolution in wheat.  
434 We have shown that microbial diversity in wheat roots grown in agricultural soil is highest in  
435 landraces bred in low-input agricultural systems. We also demonstrated that the first period after  
436 emergence of seedlings is crucial for microbial colonization of roots. Several taxa were enriched  
437 exclusively in modern or old wheat lines. Communities in both modern and old wheat lines  
438 followed the predictions of the neutral community assembly model, but ancient accessions (*Tm*  
439 and *Tt*) created more isolated environments.

440

#### 441 **Funding**

442 Funding for R.S and M.N. was provided by Independent Research Fund Denmark, grant no. 6111-  
443 00065B. M.V. was supported by the Royal Academy of Engineering under the Research  
444 Fellowship scheme.

445

#### 446 **Acknowledgements**

447 Novozymes A/S would like to acknowledge Birgitte Gjerde Bennedsen for help with the lab work.  
448 Mathilde Schiøtt Dige and Laure Boeglin, Aarhus University are likewise acknowledged for their  
449 lab work.

450

451

#### 452 **Availability of data and materials**

453 All amplicon sequencing files from this study were deposited in the NCBI sequence read archive  
454 under the accession number PRJNA611715.

455

#### 456 **References**

457 Abbasov M, Akparov Z, Gross T, *et al.* (2018) Genetic relationship of diploid wheat (*Triticum* spp.) species  
458 assessed by SSR markers. *Genetic Resources and Crop Evolution* **65**: 1441-1453.  
459 Avni R, Nave M, Barad O, *et al.* (2017) Wild emmer genome architecture and diversity elucidate wheat  
460 evolution and domestication. *Science* **357**: 93-96.  
461 Baltrus DA (2017) Adaptation, specialization, and coevolution within phytobiomes. *Curr Opin Plant Biol*  
462 **38**: 109-116.

463 Beleggia R, Rau D, Laido G, *et al.* (2016) Evolutionary Metabolomics Reveals Domestication-Associated  
464 Changes in Tetraploid Wheat Kernels. *Mol Biol Evol* **33**: 1740-1753.

465 Berendsen RL, Pieterse CMJ & Bakker PAHM (2012) The rhizosphere microbiome and plant health.  
466 *Trends Plant Sci* **17**: 478-486.

467 Bouffaud ML, Poirier MA, Muller D & Moenne-Loccoz Y (2014) Root microbiome relates to plant host  
468 evolution in maize and other Poaceae. *Environmental Microbiology* **16**: 2804-2814.

469 Brisson VL, Schmidt JE, Northen TR, Vogel JP & Gaudin ACM (2019) Impacts of Maize Domestication and  
470 Breeding on Rhizosphere Microbial Community Recruitment from a Nutrient Depleted Agricultural Soil.  
471 *Sci Rep* **9**: 15611.

472 Bulgarelli D, Garrido-Oter R, Muench PC, Weiman A, Droege J, Pan Y, McHardy AC & Schulze-Lefert P  
473 (2015) Structure and Function of the Bacterial Root Microbiota in Wild and Domesticated Barley. *Cell*  
474 *Host & Microbe* **17**: 392-403.

475 Caporaso JG, Kuczynski J, Stombaugh J, *et al.* (2010) QIIME allows analysis of high-throughput  
476 community sequencing data. *Nature Methods* **7**: 335-336.

477 Carrion VJ, Perez-Jaramillo J, Cordovez V, *et al.* (2019) Pathogen-induced activation of disease-  
478 suppressive functions in the endophytic root microbiome. *Science* **366**: 606-+.

479 Chaluvadi S & Bennetzen JL (2018) Species-Associated Differences in the Below-Ground Microbiomes of  
480 Wild and Domesticated Setaria. *Front Plant Sci* **9**.

481 Dinu M, Whittaker A, Pagliai G, Benedettelli S & Sofi F (2018) Ancient wheat species and human health:  
482 Biochemical and clinical implications. *Journal of Nutritional Biochemistry* **52**: 1-9.

483 Edwards J, Johnson C, Santos-Medellin C, Lurie E, Podishetty NK, Bhatnagar S, Eisen JA & Sundaresan V  
484 (2015) Structure, variation, and assembly of the root-associated microbiomes of rice. *P Natl Acad Sci*  
485 *USA* **112**: E911-E920.

486 Escudero-Martinez C & Bulgarelli D (2019) Tracing the evolutionary routes of plant-microbiota  
487 interactions. *Curr Opin Microbiol* **49**: 34-40.

488 Finkel OM, Castrillo G, Herrera Paredes S, Salas Gonzalez I & Dangl JL (2017) Understanding and  
489 exploiting plant beneficial microbes. *Curr Opin Plant Biol* **38**: 155-163.

490 Germida JS, Siciliano, S.D. (2001) Taxonomic diversity of bacteria associated with the roots of modern,  
491 recent and ancient wheat cultivars. *Biol Fert Soils* **33**: 410-415.

492 Harrell FE (2016) HMisc: Harrell miscellaneous. R Package. p.^pp.

493 Hassani MA, Özkurt E, Franzenburg S & Stukenbrock EH (2020) Ecological Assembly Processes of the  
494 Bacterial and Fungal Microbiota of Wild and Domesticated Wheat Species. *Phytobiomes Journal*.

495 Hetrick BAD, Wilson GWT & Cox TS (1993) Mycorrhizal dependence of modern wheat cultivars and  
496 ancestors: a synthesis. *Canadian Journal of Botany* **71**: 512-518.

497 Iannucci A, Fragasso M, Beleggia R, Nigro F & Papa R (2017) Evolution of the Crop Rhizosphere: Impact  
498 of Domestication on Root Exudates in Tetraploid Wheat (*Triticum turgidum* L.). *Front Plant Sci* **8**: 2124.

499 Ihrmark K, Bodeker ITM, Cruz-Martinez K, *et al.* (2012) New primers to amplify the fungal ITS2 region -  
500 evaluation by 454-sequencing of artificial and natural communities. *Fems Microbiol Ecol* **82**: 666-677.

501 Kapulnik Y, Kushnir, U. (1991) Growth dependency of wild, primitive and modern cultivated wheat lines  
502 on vesicular-arbuscular mycorrhiza fungi. *Euphytica* **56**: 27-36.

503 Kavamura VN, Robinson RJ, Hughes D, Clark I, Rossmann M, Melo IS, Hirsch PR, Mendes R & Mauchline  
504 TH (2020) Wheat dwarfing influences selection of the rhizosphere microbiome. *Sci Rep* **10**: 1452.

505 Kinnunen M, Gulay A, Albrechtsen HJ, Dechesne A & Smets BF (2017) Nitrotoga is selected over  
506 Nitrospira in newly assembled biofilm communities from a tap water source community at increased  
507 nitrite loading. *Environ Microbiol* **19**: 2785-2793.

508 Klindworth A, Pruesse E, Schweer T, Peplies J, Quast C, Horn M & Glockner FO (2013) Evaluation of  
509 general 16S ribosomal RNA gene PCR primers for classical and next-generation sequencing-based  
510 diversity studies. *Nucleic Acids Res* **41**: e1.

511 Kudjordjie EN, Sapkota R, Steffensen SK, Fomsgaard IS & Nicolaisen M (2019) Maize synthesized  
512 benzoxazinoids affect the host associated microbiome. *Microbiome* **7**.

513 Lancashire PD, Bleiholder H, Vandenboom T, Langeluddeke P, Stauss R, Weber E & Witzemberger A  
514 (1991) A uniform decimal code for growth-stages of crops and weeds. *Annals of Applied Biology* **119**:  
515 561-601.

516 Leff JW, Lynch RC, Kane NC & Fierer N (2017) Plant domestication and the assembly of bacterial and  
517 fungal communities associated with strains of the common sunflower, *Helianthus annuus*. *New Phytol*  
518 **214**: 412-423.

519 Lundberg DS, Lebeis SL, Paredes SH, *et al.* (2012) Defining the core *Arabidopsis thaliana* root  
520 microbiome. *Nature* **488**: 86-+.

521 McMurdie PJ & Holmes S (2013) phyloseq: an R package for reproducible interactive analysis and  
522 graphics of microbiome census data. *Plos One* **8**: e61217.

523 Mendes R, Kruijt M, de Bruijn I, *et al.* (2011) Deciphering the Rhizosphere Microbiome for Disease-  
524 Suppressive Bacteria. *Science* **332**: 1097-1100.

525 Morris A, Beck JM, Schloss PD, *et al.* (2013) Comparison of the respiratory microbiome in healthy  
526 nonsmokers and smokers. *Am J Respir Crit Care Med* **187**: 1067-1075.

527 Nunes da Rocha U, Plugge CM, George I, van Elsas JD & van Overbeek LS (2013) The rhizosphere selects  
528 for particular groups of acidobacteria and verrucomicrobia. *Plos One* **8**: e82443.

529 Peiffer JA, Spor A, Koren O, Jin Z, Tringe SG, Dangl JL, Buckler ES & Ley RE (2013) Diversity and  
530 heritability of the maize rhizosphere microbiome under field conditions. *P Natl Acad Sci USA* **110**: 6548-  
531 6553.

532 Perez-Jaramillo JE, Mendes R & Raaijmakers JM (2016) Impact of plant domestication on rhizosphere  
533 microbiome assembly and functions. *Plant Molecular Biology* **90**: 635-644.

534 Perez-Jaramillo JE, Carrion VJ, de Hollander M & Raaijmakers JM (2018) The wild side of plant  
535 microbiomes. *Microbiome* **6**: 143.

536 Perez-Jaramillo JE, Carrion VJ, Bosse M, Ferrao LFV, de Hollander M, Garcia AAF, Ramirez CA, Mendes R  
537 & Raaijmakers JM (2017) Linking rhizosphere microbiome composition of wild and domesticated  
538 *Phaseolus vulgaris* to genotypic and root phenotypic traits. *Isme J*.

539 Pont C, Leroy T, Seidel M, *et al.* (2019) Tracing the ancestry of modern bread wheats. *Nature Genetics*  
540 **51**: 905-+.

541 Poole P, Ramachandran V & Terpolilli J (2018) Rhizobia: from saprophytes to endosymbionts. *Nat Rev*  
542 *Microbiol* **16**: 291-303.

543 Quast C, Pruesse E, Yilmaz P, Gerken J, Schweer T, Yarza P, Peplies J & Glockner FO (2013) The SILVA  
544 ribosomal RNA gene database project: improved data processing and web-based tools. *Nucleic Acids Res*  
545 **41**: D590-596.

546 Rascio A, Beleggia R, Platani C, Nigro F, Codianni P, De Santis G, Rinaldi M & Fragasso M (2016)  
547 Metabolomic diversity for biochemical traits of *Triticum* sub-species. *Journal of Cereal Science* **71**: 224-  
548 229.

549 Rognes T, Flouri T, Nichols B, Quince C & Mahe F (2016) VSEARCH: a versatile open source tool for  
550 metagenomics. *PeerJ* **4**: e2584.

551 Rosindell J, Hubbell SP & Etienne RS (2011) The unified neutral theory of biodiversity and biogeography  
552 at age ten. *Trends Ecol Evol* **26**: 340-348.

553 Rossmann M, Perez-Jaramillo JE, Kavamura VN, *et al.* (2020) Multitrophic interactions in the rhizosphere  
554 microbiome of wheat: from bacteria and fungi to protists. *Fems Microbiol Ecol* **96**.

555 Sapkota R & Nicolaisen M (2018) Cropping history shapes fungal, oomycete and nematode communities  
556 in arable soils and affects cavity spot in carrot. *Agriculture Ecosystems & Environment* **257**: 120-131.

557 Sapkota R, Knorr K, Jørgensen LN, O'Hanlon KA & Nicolaisen M (2015) Host genotype is an important  
558 determinant of the cereal phyllosphere mycobiome. *New Phytol* **207**: 1134-1144.

559 Schmidt JE, Bowles TM & Gaudin ACM (2016) Using Ancient Traits to Convert Soil Health into Crop Yield:  
560 Impact of Selection on Maize Root and Rhizosphere Function. *Front Plant Sci* **7**.  
561 Shi S, Tian L, Nasir F, Li X, Li W, Tran LP & Tian C (2018) Impact of domestication on the evolution of  
562 rhizomicrobiome of rice in response to the presence of *Magnaporthe oryzae*. *Plant Physiol Biochem* **132**:  
563 156-165.  
564 Siddique AB & Unterseher M (2016) A cost-effective and efficient strategy for Illumina sequencing of  
565 fungal communities: A case study of beech endophytes identified elevation as main explanatory factor  
566 for diversity and community composition. *Fungal Ecol* **20**: 175-185.  
567 Sloan WT, Lunn M, Woodcock S, Head IM, Nee S & Curtis TP (2006) Quantifying the roles of immigration  
568 and chance in shaping prokaryote community structure. *Environ Microbiol* **8**: 732-740.  
569 Szoboszlay M, Lambers J, Chappell J, Kupper JV, Moe LA & McNear DH (2015) Comparison of root  
570 system architecture and rhizosphere microbial communities of Balsas teosinte and domesticated corn  
571 cultivars. *Soil Biol Biochem* **80**: 34-44.  
572 Tkacz A, Pini F, Turner TR, *et al.* (2020) Agricultural Selection of Wheat Has Been Shaped by Plant-  
573 Microbe Interactions. *Front Microbiol* **11**: 132.  
574 Valente J, Gerin F, Le Gouis J, Moenne-Loccoz Y & Prigent-Combaret C (2020) Ancient wheat varieties  
575 have a higher ability to interact with plant growth-promoting rhizobacteria. *Plant Cell Environ* **43**: 246-  
576 260.  
577 Vignola M, Werner D, Wade MJ, Meynet P & Davenport RJ (2018) Medium shapes the microbial  
578 community of water filters with implications for effluent quality. *Water Res* **129**: 499-508.  
579 Wagner MR, Lundberg DS, Del Rio TG, Tringe SG, Dangl JL & Mitchell-Olds T (2016) Host genotype and  
580 age shape the leaf and root microbiomes of a wild perennial plant. *Nat Commun* **7**: 12151.  
581 Wu LY, Wen CQ, Qin YJ, Yin HQ, Tu QC, Van Nostrand JD, Yuan T, Yuan MT, Deng Y & Zhou JZ (2015)  
582 Phasing amplicon sequencing on Illumina Miseq for robust environmental microbial community analysis.  
583 *Bmc Microbiology* **15**.  
584 Yin C, Hulbert SH, Schroeder KL, Mavrodi O, Mavrodi D, Dhingra A, Schillinger WF & Paulitz TC (2013)  
585 Role of bacterial communities in the natural suppression of *Rhizoctonia solani* bare patch disease of  
586 wheat (*Triticum aestivum* L.). *Appl Environ Microbiol* **79**: 7428-7438.  
587 Zachow C, Muller H, Tilcher R & Berg G (2014) Differences between the rhizosphere microbiome of *Beta*  
588 *vulgaris* ssp *maritima* - ancestor of all beet crops - and modern sugar beets. *Front Microbiol* **5**.

589

## 590 **Figures and tables**

591 **Table 1.** Triticum accessions used in this study.

592 **Table 2.** Permutation analysis of variance (PERMANOVA) of root-associated bacterial and fungal  
593 communities in the different wheat genotypes (modern cultivars, Landraces + *Tas* and ancient  
594 lines). Adonis tests were based on Bray-Curtis distance matrices using 1,000 permutations. After  
595 the initial analysis of the total dataset, bulk soil samples were removed from the dataset, and the  
596 remaining data was split into growth stage.

597 **Table 3.** Number of OTUs present in the target communities (roots), in the source community  
598 (bulk soil) and the OTUs shared between the communities and retained for the NCM analyses.  
599 Pearson correlations and migration rates are reported.

600 **Figure 1.** Upper panels: diversity indices for bacterial communities rarefied to 3,000 reads  
601 (observed richness (first 3 panels) and Shannon Diversity Index (last 3 panels)) calculated at OTU  
602 level. Lower panels: diversity indices for fungal communities rarefied to 3,000 reads (observed  
603 richness (first 3 panels) and Shannon Diversity Index (last 3 panels). BBCH10 (emergence of first  
604 leaf), BBCH12 (first leaf fully unfolded) and BBCH21 (first side shoot visible) (Lancashire et al.,  
605 1991).

606 **Figure 2.** Nonmetric multidimensional scaling (NMDS) ordination of bacterial (A) and (B) fungal  
607 community composition in bulk soil and roots of modern, landrace + Tas, and Tm and Tt wheat  
608 accession at each sampled growth stage based on Bray-Curtis distances. BBCH10 (emergence  
609 of first leaf), BBCH12 (first leaf fully unfolded) and BBCH21 (first side shoot visible) (Lancashire  
610 et al., 1991).

611 **Figure 3.** OTUs belonging to bacterial (A) and fungal (B) phyla that are differentially enriched in  
612 the roots of old cultivars ( $\log_2$ Fold change  $<0$ ) or modern cultivars ( $\log_2$ Fold change  $>0$ ). “Old  
613 accessions” depicted in this figure groups the wheat ancestors *Tm* and *Tt*, landraces and *Tas*.  
614 “Modern cultivars” groups the commercial cultivars KWS Desanto, Substance, Sheriff and Torp.  
615 BBCH10 (emergence of first leaf), BBCH12 (first leaf fully unfolded) and BBCH21 (first side shoot  
616 visible) (Lancashire et al., 1991).

617 **Figure 4.** Fit of the predicted neutral model (NCM) to observed bacterial (top panels) and fungal  
618 community (bottom panels) assembly at OTU level. The predicted occurrence frequencies for  
619 OTUs shared between bulk soil and roots in modern (A, C) and old (B, D) wheat accessions and  
620 the predicted occurrence frequencies. For the comparison, KWS Desanto, Substance, Sheriff and  
621 Torp are classified as “modern” and the rest as “old” cultivars (Table 1). OTUs that occur  
622 significantly more frequently than predicted by the model are shown in green, while those that  
623 occur less frequently than predicted are shown in red. Dashed lines represent 95% confidence  
624 intervals around the model prediction (black line),  $m$  = immigration rate,  $\rho$ =Pearson correlation.

625

#### 626 **Supplementary figures and tables**

627 **Table S1.** Sampling times. Sampling was at BBCH 10, 12 and 21. Note that accessions Metalla,  
628 TRI 1774 and Substance were sampled on later time points due to later development. BBCH10  
629 (emergence of first leaf), BBCH12 (first leaf fully unfolded) and BBCH21 (first side shoot visible)  
630 (Lancashire et al., 1991).

631 **Table S2.** Sampling and sequencing strategy. Number of bacterial and fungal reads are shown  
632 for each sample.

633 **Figure S1.** Overview of the bacterial 16S amplicon (top panels) and fungal ITS amplicon (bottom  
 634 panels) sequencing quality: (A) number of reads per sample and (B) the length of unique amplicon  
 635 sequences. Red lines represent cut-off values for removing low quality samples and sequences.

636 **Figure S2.** Rarefaction curves for (A) bacterial 16S rRNA amplicon library and (B) fungal ITS  
 637 amplicon library.

638 **Figure S3.** Nonmetric multidimensional scaling (NMDS) ordination of bacterial and fungal  
 639 community composition in bulk soil and roots of the different accessions at each growth stage  
 640 based on Bray-Curtis distances. BBCH10 (emergence of first leaf), BBCH12 (first leaf fully  
 641 unfolded) and BBCH21 (first side shoot visible) (Lancashire et al., 1991).

642 **Figure S4.** Comparison of the frequency of observation of unique genera of bacteria (A) and fungi  
 643 (B) in the roots of modern and old ('monococcum' = *Tm*, 'turgidium' = *Tt* and 'aestivum' =  
 644 landraces) wheat varieties.

645 **Figure S5.** Fungal genera significantly enriched in the roots of old accessions (log2 fold change  
 646 <0) when compared to the modern cultivars (log2 fold change >0). "Old accessions" depicted in  
 647 this figure groups the wheat ancestors *Tm* and *Tt*, landraces and *Tas*. "Modern cultivars" groups  
 648 the commercial cultivars KWS Desanto, Substance, Sheriff and Torp. BBCH10 (emergence of  
 649 first leaf), BBCH12 (first leaf fully unfolded) and BBCH21 (first side shoot visible) (Lancashire et  
 650 al., 1991).

651 **Figure S6.** Comparison of unique bacterial (A) and fungal (B) OTUs enriched differentially in  
 652 ancient and modern cultivars. "Ancient accessions" depicted in this figure groups the wheat  
 653 ancestors *Tm* and *Tt*, the chosen landraces and *Tas*. "Modern cultivars" groups the commercial  
 654 cultivars KWS Desanto, Substance, Sheriff and Torp.

655

656 **Table 1.** Triticum accessions used in this study.

Name	Accession	Genome	Category	Scientific name	Remarks	
Metalla	NGB22783	AA	<i>T. monococcum</i> ( <i>Tm</i> )	<i>T. monococcum</i> ssp <i>monococcum</i>	Cultivated Einkorn	
Einkorn	NGB22756					
TRI 1774	NGB10931			<i>T. monococcum</i> ssp <i>aegilopoides</i>		Wild Einkorn
KVL 2379	NGB4802					

Emmer	NGB8190	BBA	<i>T. turgidum</i> (Tt)	<i>T. turgidum</i> ssp <i>dicoccon</i>	Emmer
Hallets	NGB8967	BBAADD	Landrace	<i>T. aestivum</i> ssp <i>aestivum</i>	Known in UK before 1900
ALS	NGB4770				Known in Denmark in the 1940s
Kolbe	NGB7032				Known before 1900.
Lys Østpreussisk Hvede	NGB8979				Known before 1900
Square Head II	NGB5147				Known from the 1870s
Oberkulmer (selection)	NGB22516				Spelt ( <i>Tas</i> )
KWS Desanto	N/A		Modern cultivars	<i>T. aestivum</i> ssp <i>aestivum</i>	Susceptible to <i>Blumeria graminis</i> and <i>Zymoseptoria tritici</i>
Substance	N/A				Resistant to <i>Blumeria graminis</i> and <i>Zymoseptoria tritici</i> , susceptible to <i>Puccinia striiformis</i>
Sheriff	N/A				Resistant to <i>Blumeria graminis</i> , <i>Zymoseptoria tritici</i> and <i>Puccinia striiformis</i>
Torp	N/A	Susceptible to <i>Blumeria graminis</i> and <i>Zymoseptoria tritici</i>			

657

658

659 **Table 2.** Permutation analysis of variance (PERMANOVA) of root-associated bacterial and fungal  
 660 communities in the different wheat genotypes (modern cultivars, Landraces + *Tas* and ancient  
 661 lines). Adonis tests were based on Bray-Curtis distance matrices using 1000 permutations. After  
 662 the initial analysis of the total dataset, bulk soil samples were removed from the dataset, and the  
 663 remaining data was split into growth stage.

664

<b>Dataset</b>	<b>Factor</b>	<b>Df</b>	<b>Bacteria (R<sup>2</sup>)</b>	<b>Fungi (R<sup>2</sup>)</b>
Total	Bulk soil vs root	1	0.13***	0.06***
Roots	Triticum genetic group	3	0.11***	0.08***
	Growth stage (BBCH)	2	0.06***	0.05***
	Triticum genetic group * BBCH	6	0.12***	0.05***
Roots BBCH10	Triticum genetic group	3	0.23***	0.13***
Roots BBCH12	Triticum genetic group	3	0.17***	0.17***
Roots BBCH21	Triticum genetic group	3	0.34***	0.11**

665

666

667

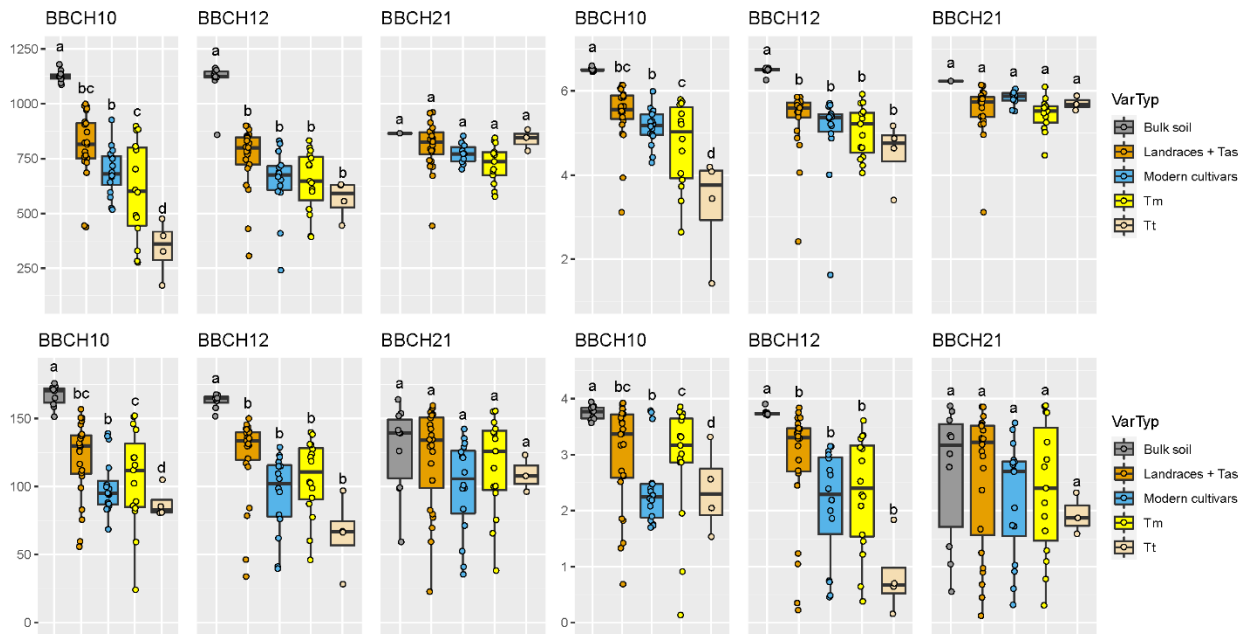
668 **Table 3.** Number of OTUs present in the target communities (roots), in the source community  
 669 (bulk soil) and the OTUs shared between the communities and retained for the NCM analyses.  
 670 Pearson correlations and migration rates are reported.

671

	Bacteria		Fungi	
	Modern	Ancient	Modern	Ancient
Target OTUs	4254	5846	318	365
Source OTUs	4539	4539	311	311
Shared OTUs	3146	3883	285	305
Pearson correlation	0.75	0.78	0.86	0.87
Migration rate (%)	7.8%	7.6%	3.0%	4.8%

672

673



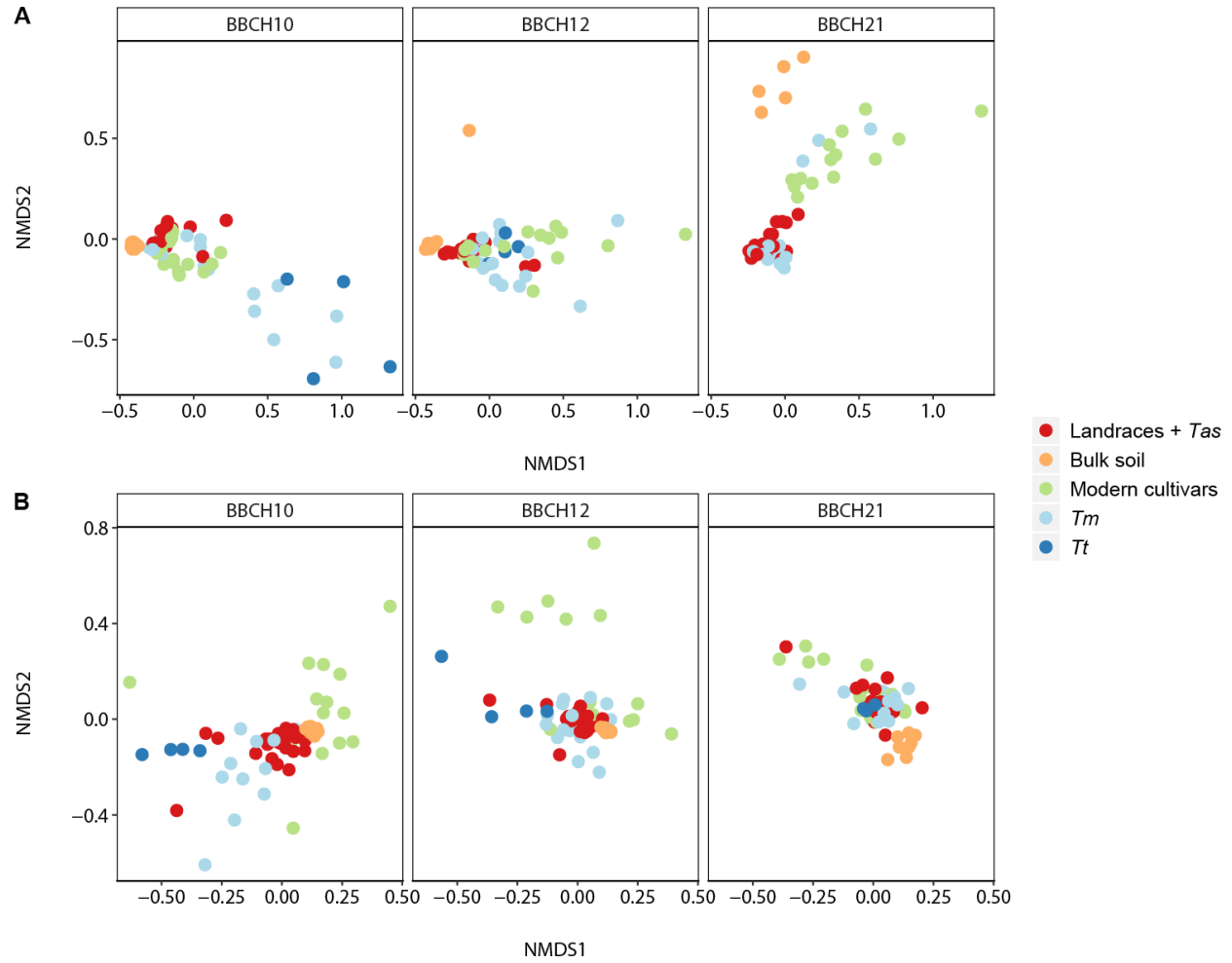
674

675 **Figure 1.** Upper panels: diversity indices for bacterial communities rarefied to 3,000 reads  
 676 (observed richness (first 3 panels) and Shannon Diversity Index (last 3 panels)) calculated at OTU  
 677 level. Lower panels: diversity indices for fungal communities rarefied to 3,000 reads (observed  
 678 richness (first 3 panels) and Shannon Diversity Index (last 3 panels)) calculated at OTU level.  
 679 BBCH10 (emergence of first leaf), BBCH12 (first leaf fully unfolded) and BBCH21 (first side shoot  
 680 visible) (Lancashire et al., 1991).

681

682

683



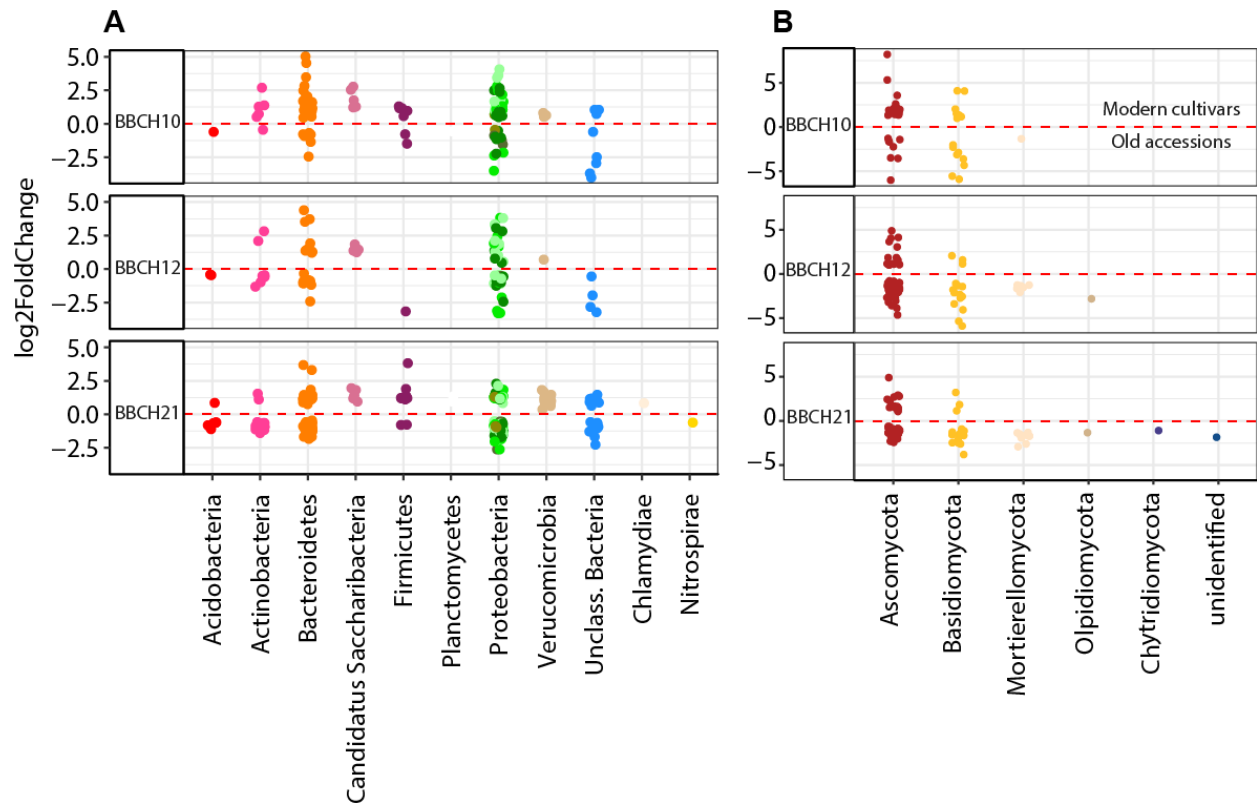
684

685 **Figure 2.** Nonmetric multidimensional scaling (NMDS) ordination of (A) bacterial and  
 686 community composition in bulk soil and roots of modern, landrace + *Tas*, and *Tm* and *Tt* wheat  
 687 accessions at each sampled growth stage based on Bray-Curtis distances. BBCH10 (emergence  
 688 of first leaf), BBCH12 (first leaf fully unfolded) and BBCH21 (first side shoot visible) (Lancashire  
 689 et al., 1991).

690

691

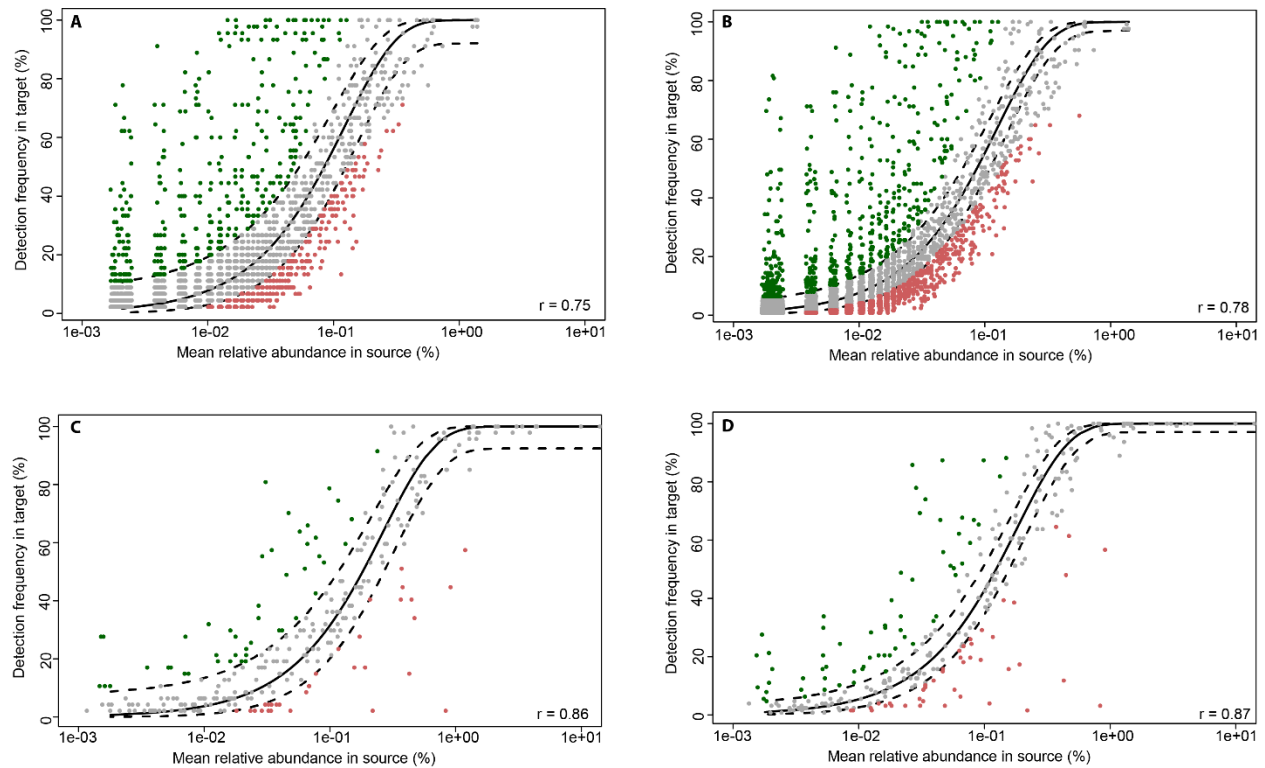
692



693  
694

695 **Figure 3.** Bacterial (A) and fungal (B) phyla differentially enriched in the roots of old cultivars  
696 (log<sub>2</sub>Fold change <0) or modern cultivars (log<sub>2</sub>Fold change >0). “Old accessions” depicted in this  
697 figure groups the wheat ancestors *Tm* and *Tt*, landraces and *Tas*. “Modern cultivars” groups the  
698 commercial cultivars KWS Desanto, Substance, Sheriff and Torp. BBCH10 (emergence of first  
699 leaf), BBCH12 (first leaf fully unfolded) and BBCH21 (first side shoot visible) (Lancashire et al.,  
700 1991).

701  
702  
703



704

705 Figure 4. Fit of the predicted neutral model (NCM) to observed bacterial (top panels) and fungal  
 706 community (bottom panels) assembly at OTU level. The predicted occurrence frequencies for  
 707 OTUs shared between bulk soil and roots in (A, C) modern and (B, D) old wheat accessions and  
 708 the predicted occurrence frequencies. For the comparison, KWS Desanto, Substance, Sheriff and  
 709 Torp are classified as “modern” and the rest as “old” cultivars (Table 1). OTUs that occur  
 710 significantly more frequently than predicted by the model are shown in green, while those that  
 711 occur less frequently than predicted are shown in red. Dashed lines represent 95% confidence  
 712 intervals around the model prediction (black line),  $r$  = Pearson correlation.

713

714 **Supplemental tables**

715

716 **Table S1.** Sampling times. Sampling was at BBCH 10, 12 and 21. Note that accessions Metalla,

717 TRI 1774 and Substance were sampled on later time points due to later development.

Accession	Name	BBCH 10	BBCH 12	BBCH 21
Bulk soil	Bulk soil	Oct 31	Nov 9	Nov 29
Nordgen NGB22783	Metalla (selection)	Nov 8	Nov 16	Dec 6
Nordgen NGB22756	Einkorn wheat, Søtofte	Oct 31	Nov 10	Nov 29
Nordgen NGB10931	TRI 1774	Nov 6	Nov 16	Dec 6
Nordgen NGB4802	KVL 2379	Oct 31	Nov 10	Nov 29
Nordgen NGB8190	Emmer	Oct 31	Nov 10	Nov 29
Nordgen NGB8967	Hallets	Oct 31	Nov 10	Nov 29
Nordgen NGB4770	ALS	Oct 31	Nov 10	Nov 29
Nordgen NGB7032	Kolbe	Oct 31	Nov 10	Nov 29
Nordgen NGB8979	Lys Østpreussisk Hvede	Oct 31	Nov 10	Nov 29
Nordgen NGB5147	SquareHead II	Oct 31	Nov 10	Nov 29
Nordgen NGB22516	Oberkulmer (selection)	Oct 31	Nov 10	Nov 29
N/A Modern cultivar	KWS Desanto	Oct 31	Nov 10	Nov 29
N/A Modern cultivar	Substance	Nov 8	Nov 16	Dec 6
N/A Modern cultivar	Sheriff	Oct 31	Nov 10	Nov 29
N/A Modern cultivar	Torp	Oct 31	Nov 10	Nov 29

718

719

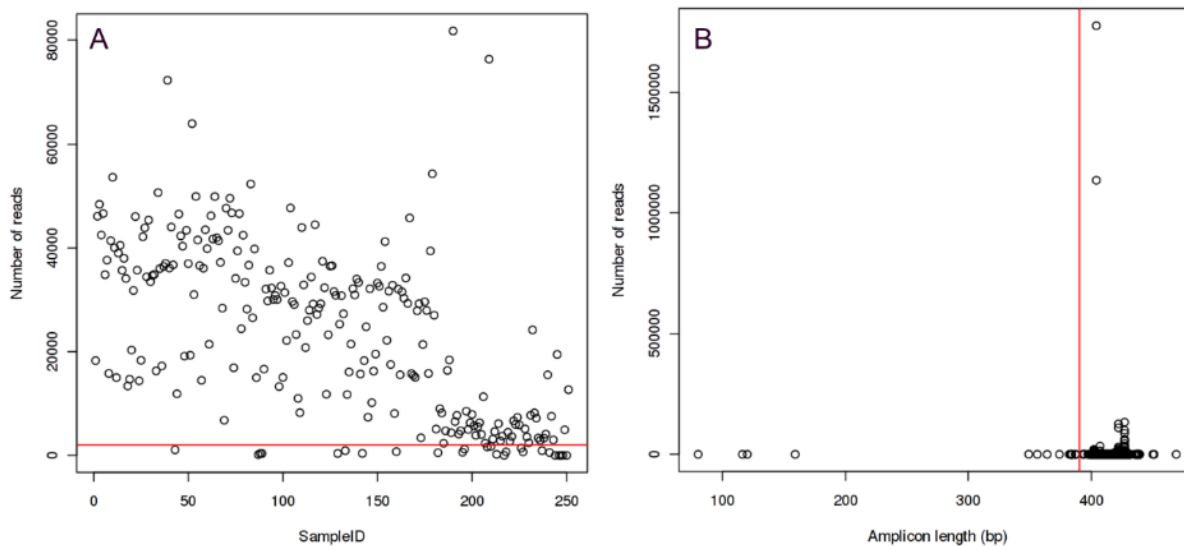
720

721 **Table S2.** Sampling and sequencing strategy. Number of bacterial and fungal reads are shown  
722 for each sample.

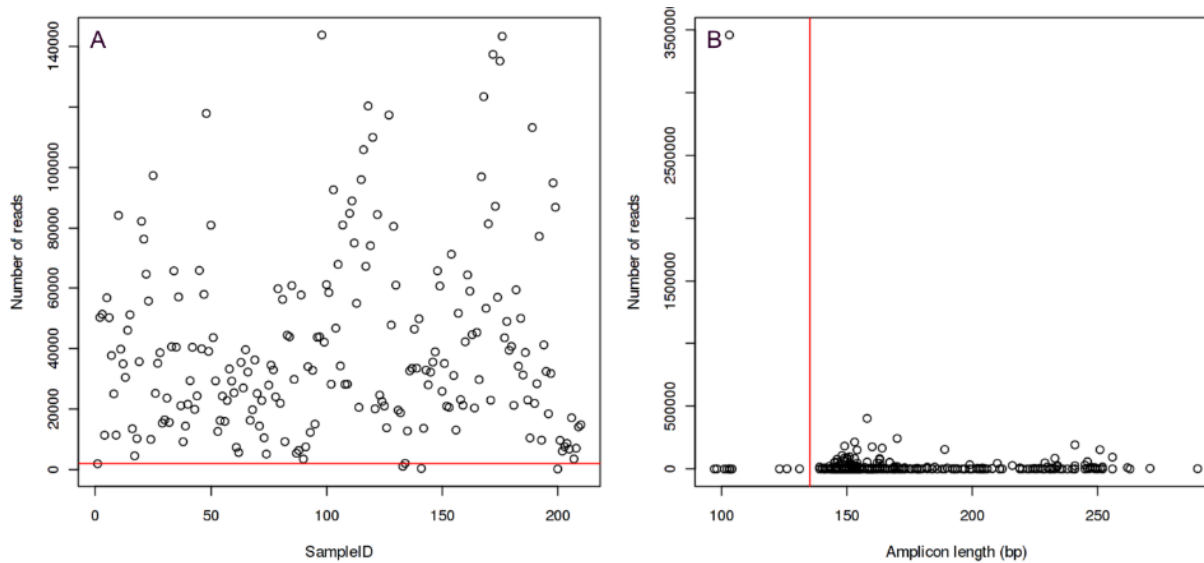
723

724 **Excel sheet**

725 **Supplementary figures**



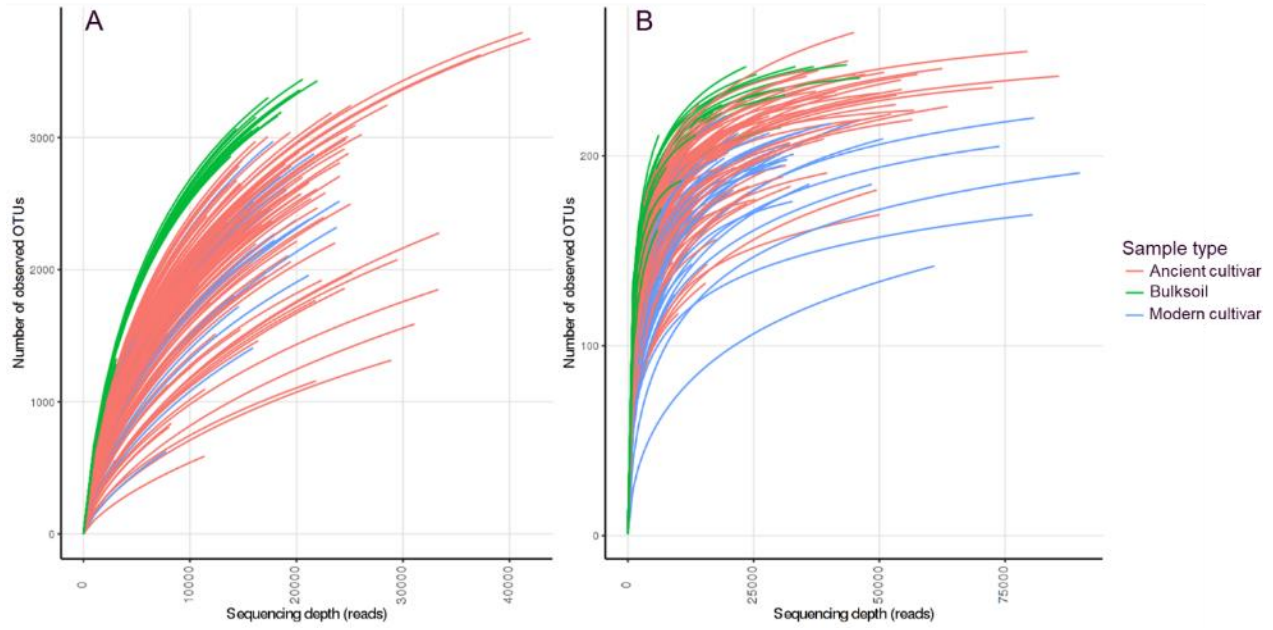
726



727

728 **Figure S1.** Overview of the bacterial 16S amplicon (top panels) and fungal ITS amplicon (bottom  
729 panels) sequencing quality: (A) number of reads per sample and (B) the length of unique amplicon  
730 sequences. Red lines represent cut-off values for removing low quality samples and sequences.

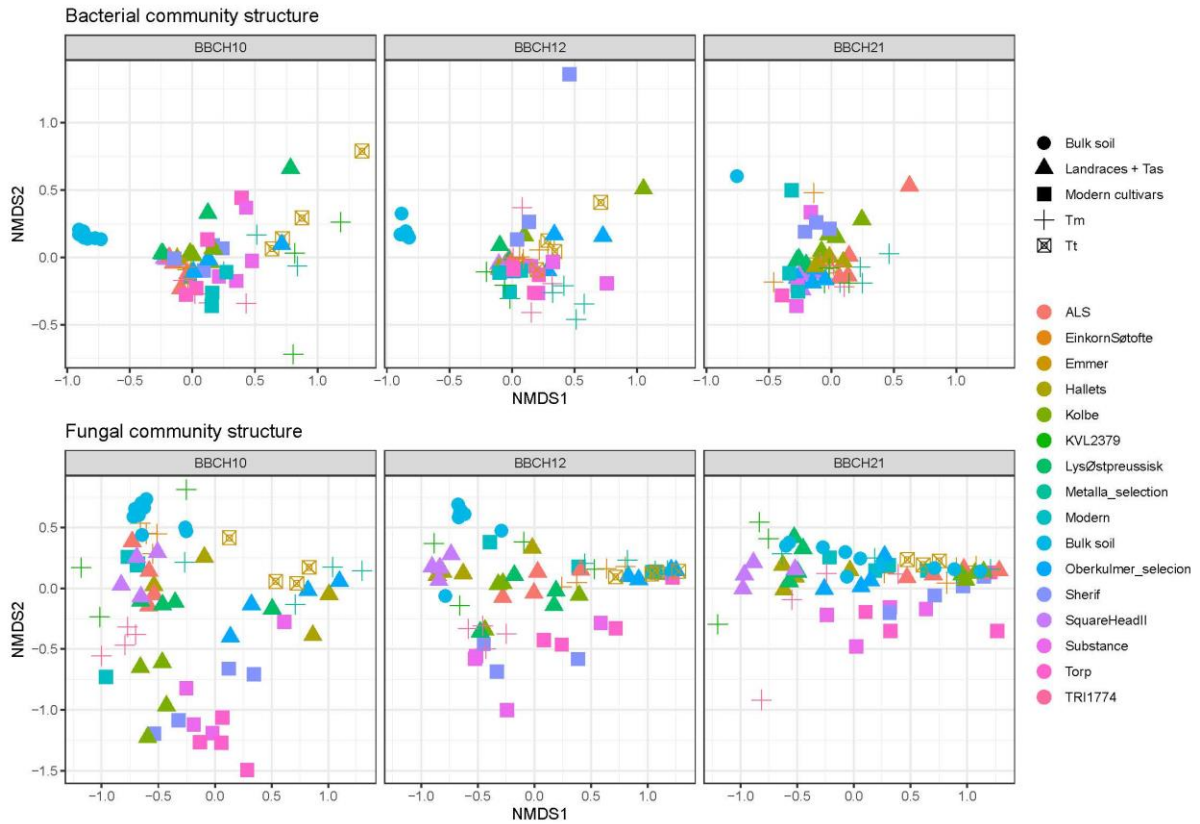
731



732

733 **Figure S2.** Rarefaction curves for (A) bacterial 16S rRNA amplicon library and (B) fungal ITS  
 734 amplicon library.

735



736

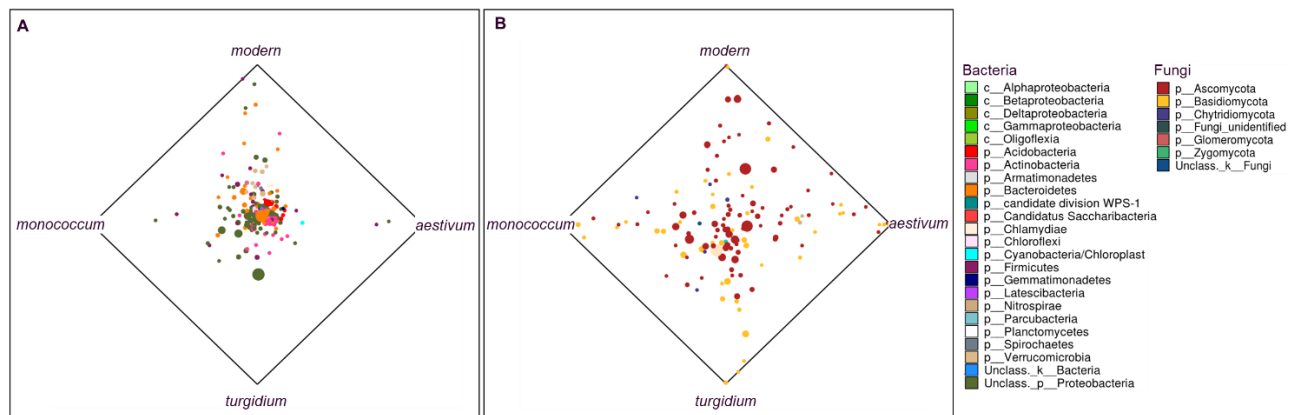
737 **Figure S3.** Nonmetric multidimensional scaling (NMDS) ordination of bacterial and fungal  
 738 community composition in bulk soil and roots of the different accessions at each growth stage  
 739 based on Bray-Curtis distances. BBCH10 (emergence of first leaf), BBCH12 (first leaf fully  
 740 unfolded) and BBCH21 (first side shoot visible) (Lancashire et al., 1991).

741

742

743

744



745

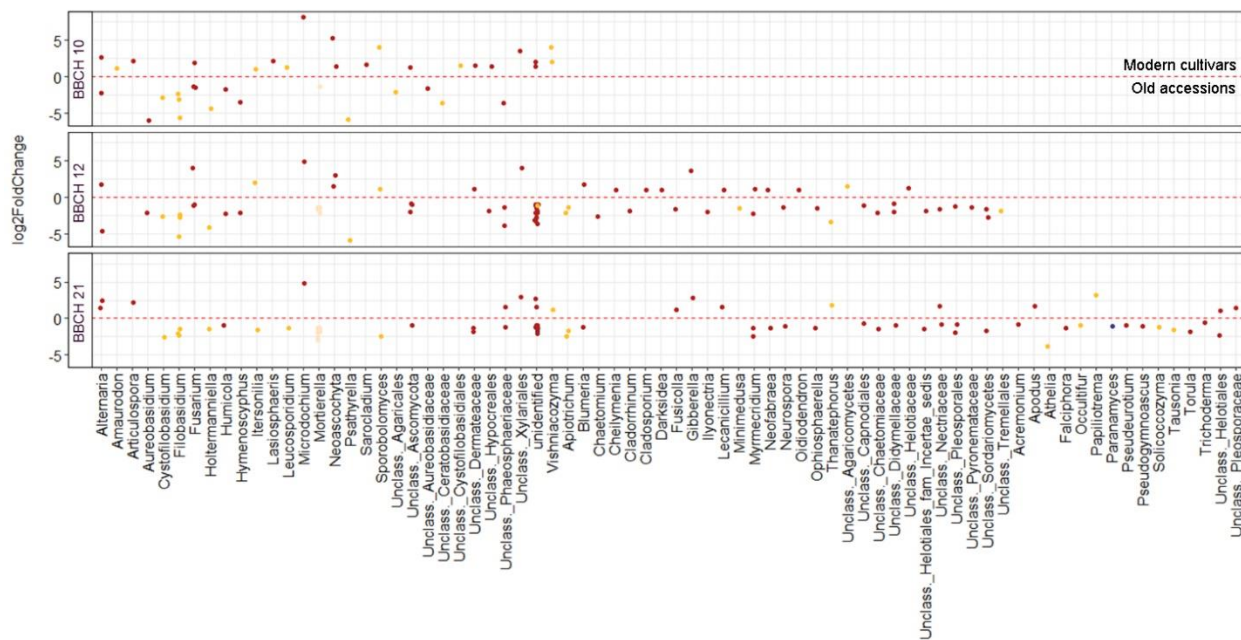
746 **Figure S4.** Comparison of the frequency of observation of unique genera of bacteria (A) and fungi

747 (B) in the roots of modern and old ('monococcum' = *Tm*, 'turgidium' = *Tt* and 'aestivum' =

748 landraces) wheat varieties.

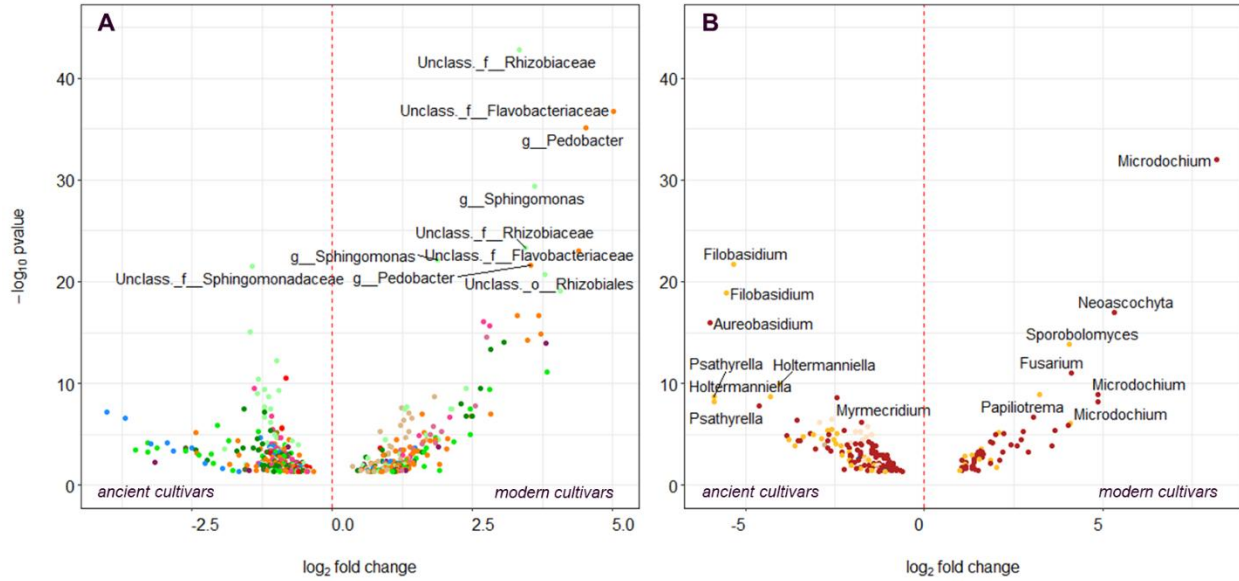
749

750  
751



752  
753  
754  
755  
756  
757

**Figure S5.** Fungal genera significantly enriched in the roots of old accessions ( $\log_2\text{Fold change} < 0$ ) when compared to the modern cultivars ( $\log_2\text{Fold change} > 0$ ). “Old accessions” depicted in this figure groups the wheat ancestors *Tm* and *Tt*, landraces and *Tas*. “Modern cultivars” groups the commercial cultivars KWS Desanto, Substance, Sheriff and Torp.



758

759

760 **Figure S6.** Comparison of unique bacterial (A) and fungal (B) OTUs enriched differentially in  
 761 ancient and modern cultivars. “Ancient accessions” depicted in this figure groups the wheat  
 762 ancestors *Tm* and *Tt*, the chosen landraces and *Tas*. “Modern cultivars” groups the commercial  
 763 cultivars KWS Desanto, Substance, Sheriff and Torp.

764

765